

# Evidence for the chaotic origin of Northern Annular Mode variability

S. M. Osprey<sup>1</sup> and M. H. P. Ambaum<sup>2</sup>

Received 18 May 2011; revised 23 June 2011; accepted 24 June 2011; published 3 August 2011.

[1] Exponential spectra are found to characterize variability of the Northern Annular Mode (NAM) for periods less than 36 days. This corresponds to the observed rounding of the autocorrelation function at lags of a few days. The characteristic persistence timescales during winter and summer is found to be  $\sim 5$  days for these high frequencies. Beyond periods of 36 days the characteristic decorrelation timescale is  $\sim 20$  days during winter and  $\sim 6$  days in summer. We conclude that the NAM cannot be described by autoregressive models for high frequencies; the spectra are more consistent with low-order chaos. We also propose that the NAM exhibits regime behaviour, however the nature of this has yet to be identified. **Citation:** Osprey, S. M., and M. H. P. Ambaum (2011), Evidence for the chaotic origin of Northern Annular Mode variability, *Geophys. Res. Lett.*, 38, L15702, doi:10.1029/2011GL048181.

## 1. Introduction

[2] Identification of distinct modes of climate variability and their characteristic timescales has been an active area of research. One particular example of this being the Northern Annular Mode (NAM) and its regional counterpart, the North Atlantic Oscillation (NAO). Previous studies of the NAO have recognised distinct behaviour over a range of timescales, prompting some to conclude that no one process can likely account for all variability [Stephenson *et al.*, 2000; Keeley *et al.*, 2009]. Previous studies link this variability to preferred states of the tropospheric jet following breaking of upper-level Rossby waves [Woollings *et al.*, 2008, 2010; Hannachi, 2010], while others link increased persistence times with the mean-latitude of the storm-tracks [Barnes *et al.*, 2010; Barnes and Hartmann, 2010]; an effect also recognised for the Southern Annular Mode [Hartmann and Lo, 1998]. Gerber and Vallis [2007], using an idealised model, found that the intraseasonal timescale of extratropical variability was not simply related to boundary layer friction or radiative timescales. They describe a feedback of the eddy-forcing on the jet which is sensitive to the longitudinal extent of the former: more pronounced localisation leads to reduced sensitivity of timescale to imposed friction and heating. In describing the NAM, other studies have recognised power-law characteristics for the low frequency spectra, providing evidence for a stochastic description [Feldstein, 2000; Vallis

*et al.*, 2004; Gerber and Vallis, 2005; Franzke and Woollings, 2011].

[3] Hasselmann [1976] provided the standard description of such noise processes in terms of a random walk (also called an AR1 process). In these processes the reddening of the spectrum is provided by memory processes which integrate the high-frequency noise. These models can be generalised to higher order noise processes, including coloured noise (e.g., ARMA processes). Clearly such models would provide better fits to the data, as they have more fitting parameters, but generally lack physical justification. Consequently, we adopt the AR1 process as the archetypal noise model.

[4] Exponential power-spectra have been identified in a number of idealised nonlinear systems and are thought to characterise low-dimensional chaos [Sigeti and Horsthemke, 1987; Sigeti, 1995b; Ohtomo *et al.*, 1995]. It is argued that these characteristics can help to differentiate deterministic low-order chaos from stochastic processes, whose power-spectra display power-law dependence [Sigeti, 1995a]. Brandstater and Swinney [1987] in annulus studies of Taylor-Couette flow, identified exponential spectra with intermittency: the transition from quasi-periodic to weakly turbulent regimes. Other examples include: non-periodic beating in heart rhythm studies [Babloyantz and Destexhe, 1988], the dynamics of flame fronts [Elhamdi *et al.*, 1993] and laboratory studies of plasmas [Pace *et al.*, 2008]. The slope of exponential spectra are thought to be largely independent of dynamics; the mathematical structure of associated timescales were explored by Frisch and Morf [1981].

[5] Here we present evidence for an exponential form of the 1000 hPa NAM power-spectrum corresponding to periods of less than 36 days and conclude that this provides support for intermittent chaos controlling NAM behaviour for periods of several weeks, at least.

[6] The paper briefly sets out describing the NAM timeseries used, before giving details of the sampling and methods used to construct time-of-year autocorrelations. We then show results of summer and winter NAM lag-autocorrelation and power-spectra, before finally providing a motivating example of the spectral characteristics of low-dimensional chaos, using the Lorenz-63 system [Lorenz, 1963].

## 2. Data and Methods

[7] Here we use NAM timeseries data for the period 1958–2001 as compiled for and outlined by Baldwin and Dunkerton [2001], and extended through to July 2006 (<http://www.nwra.com/resumes/baldwin/nam.php>). In summary, this comprises the principal component timeseries of the leading empirical orthogonal function (EOF) of deseasonalised zonal mean daily 1000 hPa geopotential height. The EOF is defined between 20°N–90°N, on 90-day smoothed time-

<sup>1</sup>National Center for Atmospheric Science, Department of Physics, University of Oxford, Oxford, UK.

<sup>2</sup>Department of Meteorology, University of Reading, Reading, UK.

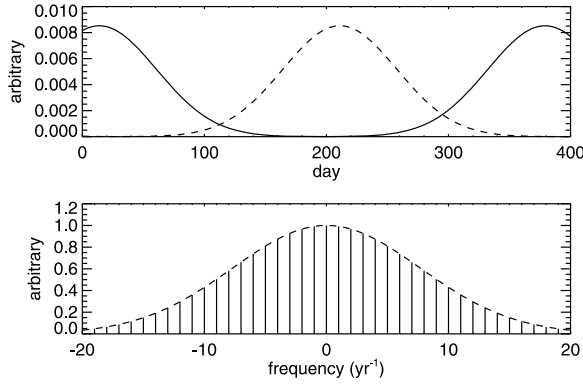


**Figure 1.** (top) The filter used to sift NCEP NAM time series for the calculation of time-of-year autocorrelation and (bottom) its corresponding Fourier transform. See (2) and text for details.

series between November–March. NAM anomalies were calculated by projecting the original deseasonalised time-series onto the EOF.

[8] A filter  $m$  is used to calculate the time-of-year lag-autocorrelation function  $\rho(\tau; t')$ , where  $t'$  is a particular time of year and  $\tau$  is lag. The idealised filter is constructed following the convolution of a Gaussian of unit area ( $g$ ) with a repeating Dirac-delta function (comb-filter); the latter being defined as

$$\text{III}(t; t') \equiv \sum_{n=0}^{N-1} \delta(t - t' - Dn), \quad 0 < t' < D \quad (1)$$

centred on  $t'$ , repeated every  $D = 365$  days for  $N$  years. The Gaussian ( $g$ ) is chosen with a standard deviation  $\sigma$  of 50 days, to achieve an adequate sampling within summer and winter, while maintaining a distinction between seasons. The filter is defined as

$$m(t; t') = \int_{-\infty}^{\infty} g(u) \text{III}(t - u; t') du \doteq g * \text{III} \quad (2)$$

where, for future expedience, we introduce the convolution operator by way of an asterisk in the final term. Our measure for the *time-of-year* autocovariance  $R(\tau; t')$  is found by correlating the unfiltered and filtered NAM time series,  $z$ :

$$R(\tau; t') = \int_{-\infty}^{\infty} m(t; t') z(t) z(t + \tau) dt \doteq m z * z \quad (3)$$

Here we have defined the autocovariance operator using a star on the right of the equation. Associated with  $R$  is a local measure of the power spectrum for the daily NAM ( $P$ ) which follows from the Wiener-Khinchine Theorem [Wiener, 1930; Khinchine, 1934]. This theorem states that the autocovariance function of a data series is equal to the inverse Fourier transform of the series' power spectrum. In the present context,

$$\begin{aligned} P(f; t') &= \mathcal{F}(R(\tau; t')) \\ &= (M * Z) Z^* \\ &= (\text{III}_f * Z) Z^* \end{aligned} \quad (4)$$

where the upper-case parameters are the Fourier transforms of their lower-case equivalents, and where  $\mathcal{F}$  represents the Fourier transform. A degree of symmetry is found between the masking function  $m$  and its Fourier transform  $M$ , i.e. the Fourier transform of  $g$  ( $G$ ) is itself a Gaussian, while  $\text{III}$  is associated with a similar sifting function in the frequency domain ( $\text{III}_f$ ), with a discrete spacing of  $1 \text{ year}^{-1}$ . The masking function  $m$  and its transform  $M$  are shown in Figure 1.

[9] The influence of the masking function on  $P$  can be inferred from (1) and (4). In the limit as  $D \rightarrow \infty$ ,  $G \text{III}_f \rightarrow G$ . This is tantamount to sampling the original data about *one* region centred on  $t'$ . The convolution in (4) smooths power across a range of frequencies. For a red spectrum, power is redistributed from low to high frequencies, resulting in a *broadened* spectrum. This engenders a complimentary response in  $R$ , which can be understood from the Fourier *Reciprocity Principle*:

$$\Delta R \Delta P = 1 \quad (5)$$

which states that the characteristic timescale (autocorrelation-width) of the autocovariance function,  $\Delta R$ , is equal to the inverse of the equivalent band-width of the power-spectrum,  $\Delta P$ . Consequently, if sampling broadens the peak in  $P$  at low frequencies, there must be a corresponding sharpening in the autocovariance function  $R$  at small lag. This naturally explains results from previous studies showing reduced levels of autocorrelation in finite-length data [Trenberth, 1984].

[10] For this study, we retrieve  $R$  for the 1000 hPa NAM by fitting a piecewise function to the power-spectrum,  $P$ , before inverting using (4). Firstly, we are guided to fit a Lorentzian to the low frequency part of  $P$  ( $\omega < \omega_c$ ), as this corresponds to exponential decay at large lag in  $R$ , a characteristic of stochastic variability of an AR1 process, but is also linked with high dimensional chaos. We then fit an exponential function to high wavenumbers ( $\omega \geq \omega_c$ ) as this characterises the presence of chaos in many low-dimensional systems. Specifically we do a least squares fit of  $P$  to

$$P_{\text{fit}}(\omega; t') = \begin{cases} 2A\alpha(\alpha^2 + \omega^2)^{-1} & : \omega < \omega_c \\ B \exp(-\beta\omega/2) & : \omega \geq \omega_c \end{cases} \quad (6)$$

Here we identify  $A$  and  $B$  as the integrated power and  $\alpha$  and  $\beta$  as characteristic frequency scales, for the low and high frequency fits, respectively. The cross-over frequency  $\omega_c$  is chosen to minimise any discontinuity between the two retrieved fits. The autocovariance function is calculated from inverting (4), above. This supports our choice of minimising the misfit of  $P_{\text{fit}}(\omega_c)$ , as any significant discontinuity would introduce spurious numerical features following the inversion of (4). The time-of-year fitted autocorrelation function  $\rho_{\text{fit}}(\tau; t')$  is defined as the ratio of the autocovariance function to its value at zero-lag:

$$\rho_{\text{fit}}(\tau; t') = R_{\text{fit}}(\tau; t') / R_{\text{fit}}(0; t') \quad (7)$$

[11] Finally we define a width measure for the two portions of  $P_{\text{fit}}$  using equivalent width as described by *Bracewell* [1978], namely,

$$\Delta P_{\text{fit}} = \int_{-\infty}^{\infty} P_{\text{fit}}(f; t') d\tau / P_{\text{fit}}(0; t') \quad (8)$$

where we use values extrapolated over the *entire* frequency domain for each of the fits. Using (5), we can then calculate an autocorrelation timescale for low and high frequency portions of the spectra. We find that the autocorrelation timescales retrieved for low and high frequencies are  $(1 - \alpha)^{-1}$  and  $\beta\pi/4$ , respectively. Uncertainty estimates (standard deviations) are calculated by varying  $\omega_c$  within the range  $5 < \omega_c < 15$  for winter and  $20 < \omega_c < 40$  for summer.

### 3. Results

[12] Figure 2 shows power spectra of the filtered summer and winter NAM time series on a semi-log scale. The winter period is centred on January 15 while the summer period is centred on July 15. The results show little sensitivity to the precise specification of dates around mid-summer and mid-winter. Both spectra show broadband structure and enhanced power at low frequencies, with the wintertime NAM spectra exhibiting greater variance across all frequencies. The summertime spectrum exhibits a linear decrease in log-power at high frequencies ( $\omega > \omega_c = 30 \times 2\pi \text{ year}^{-1}$ ), as shown on the semi-log scale, and is well described by an exponential whose corresponding autocorrelation width  $\Delta\rho$  is  $(4.66 \pm 0.04)$  days. At frequencies lower than  $\omega_c$ , even though the spectral shape is Lorentzian, the retrieved timescale is  $(5.94 \pm 0.05)$  days. The wintertime NAM spectra exhibits distinct structure at high and low frequencies. Frequencies greater than  $\omega = 10 \times 2\pi \text{ yr}^{-1}$ , equivalent to a period of 36 days, show a similar exponential relationship to those in summer, with a decay constant of  $(4.63 \pm 0.04)$  days. At lower frequencies, the slope of the spectrum is steeper indicating a time scale of  $(20.64 \pm 1.32)$  days.

[13] Also shown in Figure 2 are AR1 fits to the summer and winter spectra, computed over all frequencies. It is seen that although the fit is good over low frequencies during winter and low-mid frequencies during summer, it is generally poor elsewhere. At high frequencies the AR1 fit shall

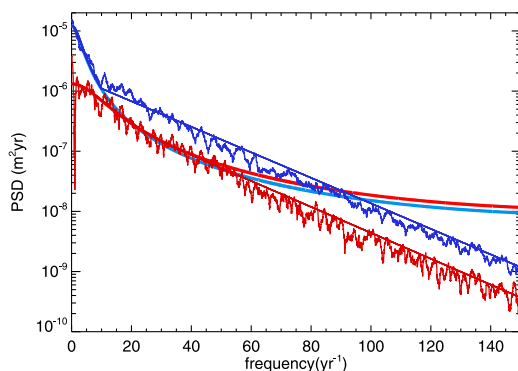


**Figure 2.** Representative NCEP Power spectra for summer (red) and winter (blue). Lorentzian fits are made at low frequencies ( $0 < \omega < \omega_c$ ) for both summer ( $\omega_c = 30 \times 2\pi \text{ yr}^{-1}$ ) and winter ( $\omega_c = 10 \times 2\pi \text{ yr}^{-1}$ ). Exponential fits are made for  $\omega > \omega_c$ . Also shown are Lorentzian fits extending over all frequencies, characteristic of AR1 processes (thick lines). For clarity a spectral smoothing is made using a spectral window of width  $1 \times 2\pi \text{ yr}^{-1}$ .

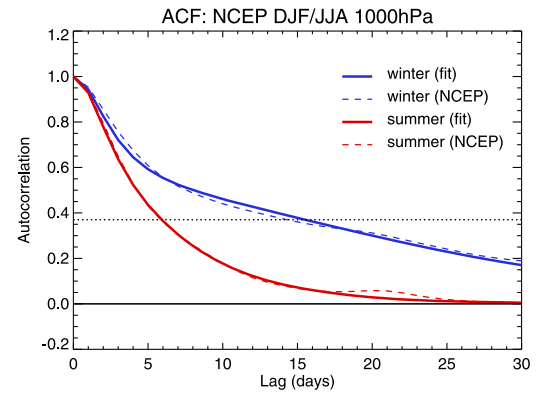


**Figure 3.** Representative NCEP autocorrelations for summer (red) and winter (blue). Observed values (dashed) are compared with the retrieved estimates of  $\rho_{\text{fit}}$  (thick) following inversion of  $P_{\text{fit}}$  using (4).

ows, which is characteristic of power-law spectra, in stark contrast to the observed spectra and the exponential fits.

[14] The summer and winter observed ( $\rho$ ) and fitted ( $\rho_{\text{fit}}$ ) NAM autocorrelations are shown in Figure 3. The observed  $\rho$  for summer and winter shows a rounding off at lags less than 2 days, and is consistent with day-to-day persistence, while the steeper slope at longer lag-times is associated with the breakdown of this persistence due to broadband natural variability. A noticeable reduction in the slope of the winter autocorrelation function is seen beyond 6 days. This is directly linked with the piecewise structure found in the winter NAM spectra. This has been associated with a “shouldering” feature in previous studies, most noticeable near 20 days [Ambaum and Hoskins, 2002; Norton, 2003]. A similar feature is seen during summer at 20 days, although unlike winter, it is accompanied by a continued rapid decrease in the background.

### 4. Discussion and Conclusion

[15] Power-law relationships describing the low frequency NAM variability can be found throughout the literature, though it is not apparent why such a description should be applicable at high frequencies. Arguments against this are outlined by Sigeti and Horsthemke [1987]. They reason that time series of deterministic systems can be differentiated to arbitrary order, unlike time series from stochastic processes. They state that the power-spectra of stochastic processes can only be described by a finite order power-law of the type  $\omega^{-2n}$  ( $n \in \mathcal{I}^+$ ) and so cannot decay at high frequency as fast as exponentially distributed spectra. The existence of an exponential relationship describing the summertime NAM and timescales shorter than  $\sim 36$  days during wintertime, suggests characteristics beyond simple power-law descriptions of underlying stochastic variability. Sigeti [1995b] shows that the slope of an exponential spectrum (in our case  $\sim 5 \text{ days}^{-1}$ ) is proportional to the sum of the positive Lyapunov exponents (a defining characteristic of chaos), and thus related to the short term error growth of a dynamical system.

[16] To explore the origins of the exponential characteristics of high-frequency NAM variability we examine the autocorrelation and spectral characteristics of the Lorenz-63

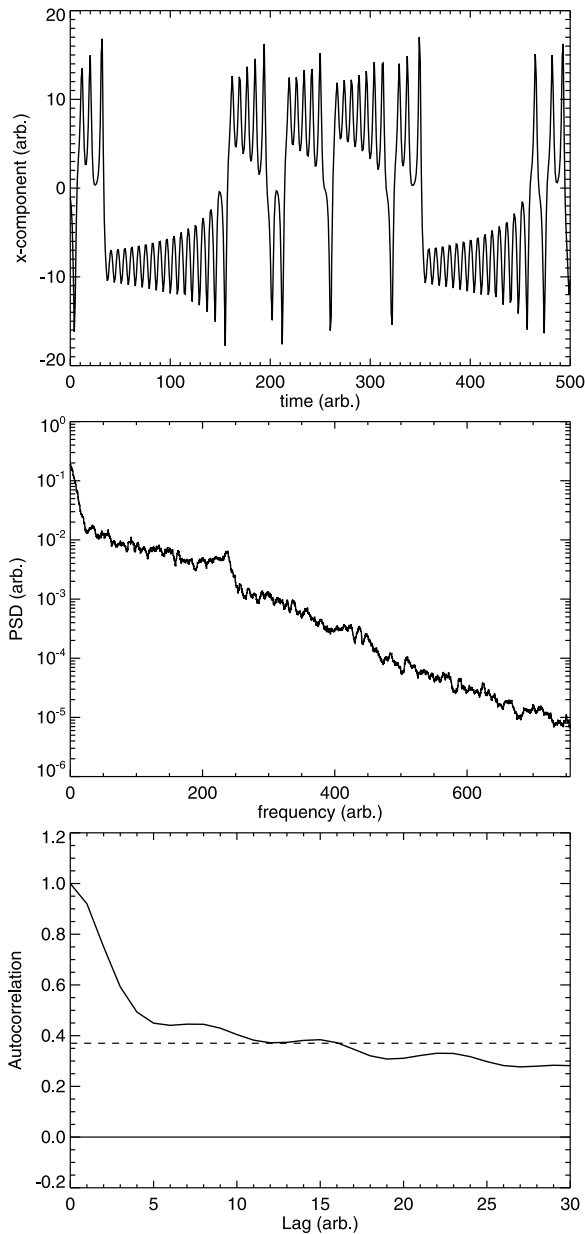


**Figure 4.** A numerical integration of the Lorenz-63 system showing (top) timeseries, (middle) power-spectra, and (bottom) autocorrelation function. The time unit scale has been adjusted for comparison with previous results. Units are otherwise arbitrary.

system – the classic example of a simple system exhibiting chaos [Lorenz, 1963]. We define the following:

$$\begin{aligned}\dot{x} &= \sigma y - \sigma x \\ \dot{y} &= x(R - z) - y \\ \dot{z} &= xy - bz\end{aligned}\quad (9)$$

The values for the parameters are taken from Lorenz [1963], that is:  $\sigma = 10.0$ ,  $R = 28.0$  and  $b = 8/3$ . The equations were solved using a fourth-order Runge-Kutta scheme for 2000 model time units, sampled once every 0.1 time units.

[17] Figure 4 shows a portion of the x-component time series, together with the autocorrelation function,  $\rho_{Lz}$  and

power-spectra,  $P_{Lz}$ . The time series shows two types of vacillation behaviour *around* individual and *between* two fixed-points in phase-space. The power-spectrum  $P_{Lz}$  shows the signature of the former, with a peak occurring around 200–250 cycles. The expression of the latter is shown as enhanced power at low frequency (<50 cycles). The other conspicuous feature within the spectra is the broadband exponential slope seen at frequencies >50 cycles. The autocorrelation function  $\rho_{Lz}$  shows a weak drop in value <2 time units, followed by a steep drop in value until 5 time units before, falling off more slowly at greater lags. The presence of the vacillations around the individual fixed points shows up as an oscillation in  $\rho_{Lz}$  with a period of 7 time units.

[18] Our analysis demonstrates that the wintertime NAM at low frequencies ( $1/f > 36$  days) has more power than what would be expected from an extrapolation of the high-frequency exponential spectrum evident at high frequencies. These characteristics are also evident in the Lorenz-63 system and are in this case linked with the existence of fixed (saddle) points and a strange-attractor in phase space. Evidence of such dense points for the NAM is debated and it is fair to say that there is currently no consensus on their existence or absence.

[19] The excess variance at low frequencies can be interpreted as a definition of regimes in the time domain. In this definition, a regime is simply a longer than expected period (compared to some homogeneous in frequency null-hypothesis - e.g., a low order chaotic model) where the NAM persists around some value. This need not correspond to a fixed point of some lower order chaotic system, and so the “regimes” would not correspond to fixed patterns in real space or state space (or values, in the case of the NAM).

[20] The presence of exponential spectra for high frequencies suggests that deterministic chaos dominates the high-frequency ( $1/f < 36$  days) NAM variability. This suggests one should exercise caution before interpreting the dynamics of the NAM as being stochastic in origin. Although such concepts can be useful in parameterising the long-range effects of chaotic variability, they can be misleading in diagnosing mechanisms for short-term and seasonal predictability.

[21] **Acknowledgments.** We thank M. Baldwin for providing the NCEP derived NAM data for this project and also the thoughtful and constructive comments from two anonymous reviewers.

[22] The Editor wishes to acknowledge Christian Franzke and an anonymous reviewer for their assistance evaluating this manuscript.

## References

- Ambaum, M., and B. Hoskins (2002), The NAO troposphere-stratosphere connection, *J. Clim.*, *15*(14), 1969–1978.
- Babloyantz, A., and A. Destexhe (1988), Is the normal heart a periodic oscillator, *Biol. Cybern.*, *58*(3), 203–211.
- Baldwin, M., and T. Dunkerton (2001), Stratospheric harbingers of anomalous weather regimes, *Science*, *294*(5542), 581–584.
- Barnes, E. A., and D. L. Hartmann (2010), Testing a theory for the effect of latitude on the persistence of eddy-driven jets using CMIP3 simulations, *Geophys. Res. Lett.*, *37*, L15801, doi:10.1029/2010GL044144.
- Barnes, E. A., D. L. Hartmann, D. M. W. Frierson, and J. Kidston (2010), Effect of latitude on the persistence of eddy-driven jets, *Geophys. Res. Lett.*, *37*, L11804, doi:10.1029/2010GL043199.
- Bracewell, R. (1978), *The Fourier Transform and its Applications*, McGraw-Hill, New York.
- Brandstater, A., and H. Swinney (1987), Strange attractors in weakly turbulent couette-taylor flow, *Phys. Rev. A*, *35*(5), 2207–2220.
- Elhamdi, M., M. Gorman, and K. Robbins (1993), Deterministic chaos in laminar premixed flames—Experimental classification of chaotic dynamics, *Combust. Sci. Technol.*, *94*(1–6), 87–101.

- Feldstein, S. (2000), The timescale, power spectra, and climate noise properties of teleconnection patterns, *J. Clim.*, *13*(24), 4430–4440.
- Franzke, C., and T. Woollings (2011), On the persistence and predictability properties of North Atlantic climate variability, *J. Clim.*, *24*(2), 466–472, doi:10.1175/2010JCLI3739.1.
- Frisch, U., and R. Morf (1981), Intermittency in non-linear dynamics and singularities at complex times, *Phys. Rev. A*, *23*(5), 2673–2705.
- Gerber, E., and G. Vallis (2005), A stochastic model for the spatial structure of annular patterns of variability and the North Atlantic Oscillation, *J. Clim.*, *18*(12), 2102–2118.
- Gerber, E. P., and G. K. Vallis (2007), Eddy-zonal flow interactions and the persistence of the zonal index, *J. Atmos. Sci.*, *64*(9), 3296–3311, doi:10.1175/JAS4006.1.
- Hannachi, A. (2010), On the origin of planetary-scale extratropical winter circulation regimes, *J. Atmos. Sci.*, *67*(5), 1382–1401, doi:10.1175/2009JAS3296.1.
- Hartmann, D., and F. Lo (1998), Wave-driven zonal flow vacillation in the Southern Hemisphere, *J. Atmos. Sci.*, *55*(8), 1303–1315.
- Hasselmann, K. (1976), Stochastic climate models part i. Theory, *Tellus*, *28*(6), 473–485, doi:10.1111/j.2153-3490.1976.tb00696.x.
- Keeley, S. P. E., R. T. Sutton, and L. C. Shaffrey (2009), Does the North Atlantic Oscillation show unusual persistence on intraseasonal time-scales?, *Geophys. Res. Lett.*, *36*, L22706, doi:10.1029/2009GL040367.
- Khintchine, A. (1934), Korrelationstheorie der stationären prozesse, *Math. Ann.*, *109*, 604–615.
- Lorenz, E. (1963), Deterministic nonperiodic flow, *J. Atmos. Sci.*, *20*(2), 130–141.
- Norton, W. (2003), Sensitivity of northern hemisphere surface climate to simulation of the stratospheric polar vortex, *Geophys. Res. Lett.*, *30*(12), 1627, doi:10.1029/2003GL016958.
- Ohtomo, N., K. Tokiwano, Y. Tanaka, A. Sumi, S. Terachi, and H. Konno (1995), Exponential characteristics of power spectral densities caused by chaotic phenomena, *J. Phys. Soc. Jpn.*, *64*(4), 1104–1113.
- Pace, D. C., M. Shi, J. E. Maggs, G. J. Morales, and T. A. Carter (2008), Exponential frequency spectrum in magnetized plasmas, *Phys. Rev. Lett.*, *101*(8), 085001, doi:10.1103/PhysRevLett.101.085001.
- Sigeti, D. (1995a), Survival of deterministic dynamics in the presence of noise and the exponential decay of power spectra at high-frequency, *Phys. Rev. E*, *52*(3), 2443–2457.
- Sigeti, D. (1995b), Exponential decay of power spectra at high-frequency and positive lyapunov exponents, *Physica D*, *82*(1–2), 136–153.
- Sigeti, D., and W. Horsthemke (1987), High-frequency power spectra for systems subject to noise, *Phys. Rev. A*, *35*(5), 2276–2282.
- Stephenson, D., V. Pavan, and R. Bojariu (2000), Is the North Atlantic Oscillation a random walk?, *Int. J. Climatol.*, *20*(1), 1–18.
- Trenberth, K. E. (1984), Some effects of finite-sample size and persistence on meteorological statistics. I. Autocorrelations, *Mon. Weather Rev.*, *112*(12), 2359–2368.
- Vallis, G., E. Gerber, P. Kushner, and B. Cash (2004), A mechanism and simple dynamical model of the North Atlantic Oscillation and annular modes, *J. Atmos. Sci.*, *61*(3), 264–280.
- Wiener, N. (1930), Generalised harmonic analysis, *Acta Math.*, *55*, 117–258.
- Woollings, T., B. Hoskins, M. Blackburn, and P. Berrisford (2008), A new Rossby wave-breaking interpretation of the North Atlantic Oscillation, *J. Atmos. Sci.*, *65*(2), 609–626, doi:10.1175/2007JAS2347.1.
- Woollings, T., A. Hannachi, B. Hoskins, and A. Turner (2010), A regime view of the North Atlantic Oscillation and its response to anthropogenic forcing, *J. Clim.*, *23*(6), 1291–1307, doi:10.1175/2009JCLI3087.1.

---

M. H. P. Ambaum, Department of Meteorology, University of Reading, Reading RG6 6BB, UK.

S. M. Osprey, National Center for Atmospheric Science, Department of Physics, University of Oxford, Oxford OX1 3PU, UK. (s.osprey@physics.ox.ac.uk)